HHS Public Access

Author manuscript

J Am Chem Soc. Author manuscript; available in PMC 2018 June 14.

Published in final edited form as:

J Am Chem Soc. 2017 June 14; 139(23): 7761–7767. doi:10.1021/jacs.7b00569.

Direct Hyperpolarization of Nitrogen-15 in Aqueous Media with Parahydrogen in Reversible Exchange

Johannes F. P. Colell[a], **Meike Emondts**[b], **Angus W. J. Logan**[a], **Kun Shen**[a], **Junu Bae**[a], **Roman V. Shchepin**[c], **Gerardo X. Ortiz**[a], **Peter Spannring**[d], **Qiu Wang**[a], **Steven J. Malcolmson**[a], **Eduard Y Chekmenev**[c,e], **Martin C. Feiters**[d], **Floris P. J. T. Rutjes**[d], **Bernhard Blümich**[b,*], **Thomas Theis**[a,*], and **Warren S. Warren**[a,f,*]

[a]Department of Chemistry, Duke University, Durham, NC 27708, USA [b]Institute for Technical und Macromolecular Chemistry, RWTH Aachen University, Worringerweg 2, 52072 Aachen, Germany [c]Departments of Radiology and Biomedical Engineering, Vanderbilt Institute of Imaging Science (VUIIS), Vanderbilt Ingram Cancer Center (VICC), Vanderbilt University, Nashville, TN 37232, USA [d]Institute for Molecules and Materials, Radboud University, Heyendaalseweg 135, 6525 AJ Nijmegen, The Netherlands [e]Departments of Physics, Radiology and Biomedical Engineering, Russian Academy of Sciences, Moscow, Russia [f]Departments of Physics, Radiology and Biomedical Engineering, Duke University, Durham, NC 27707, USA

Abstract

Signal Amplification By Reversible Exchange (SABRE) is an inexpensive, fast, and even continuous hyperpolarization technique that uses para-hydrogen as hyperpolarization source. However, current SABRE faces a number of stumbling blocks for translation to biochemical and clinical settings. Difficulties include inefficient polarization in in water, relatively short lived ^{1}H-polarization, and relatively limited substrate scope. Here we use a water soluble polarization transfer catalyst to hyperpolarize nitrogen-15 in a variety of molecules with SABRE-SHEATH (SABRE in Shield Enables Alignment Transfer to Heteronuclei). This strategy works in pure H_2O or D_2O solutions, on substrates that could not be hyperpolarized in traditional ^{1}H-SABRE experiments, and we record ^{15}N T_1 relaxation times of up to 2 min.

Graphical abstract

Corresponding Authors. thomas.theis@duke.edu, warren.warren@duke.edu, bluemich@itmc.rwth-aachen.de.

ASSOCIATED CONTENT

Electronic Supplementary Information (ESI) available: Relaxation time measurements, detailed description of experimental procedures, spectral data, physicochemical reference data for H_2O. This material is available free of charge via the Internet at http://pubs.acs.org.

Author Contributions

All authors have given approval to the final version of the manuscript.

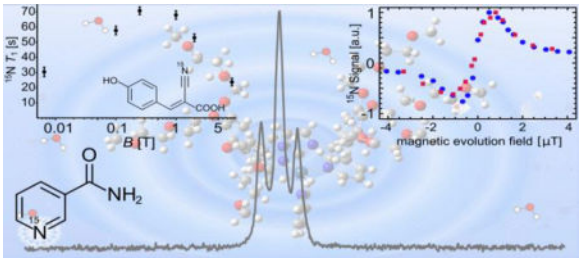

Introduction

NMR and MRI are non-destructive methods to obtain information about molecular structure and spatial morphology. However, magnetic resonance is restricted mainly because of the inherently low sensitivity as a result of low thermal polarization levels. For example, NMR spectroscopy and clinical MRI predominantly use highly abundant ^{1}H nuclei. Even so observation of low concentration analytes remains challenging. Hyperpolarization methods (e.g. DNP, PHIP, SABRE, SEOP)[1–7] enhance MR signals by 4–5 orders of magnitude and overcome inherent sensitivity limitations.[8–11]

Traditionally, hyperpolarization methods require extensive optimization. Usually methods and optimization are associated with high experimental complexity and cost. In this regard, Signal Amplification By Reversible Exchange (SABRE) stands out because it is simple, fast and continuously repeatable.[4, 12] SABRE uses readily available *para*-hydrogen (p-H_2) as source of polarization. The transfer occurs in reversibly formed substrate-hydrogen adducts in a transition metal complex. The magnetic evolution field B_{evo} must be sufficiently low to mix energy levels between hydride-^{1}H and the target nucleus to establish a path for polarization transfer.[7, 13] While protons in the substrate are targeted at magnetic fields around 65 G,[14] transfer to heteronuclei (e.g. ^{15}N, ^{13}C, ^{31}P) occurs at μT magnetic fields using a technique termed SABRE in Shield Enables Alignment Transfer to Heteronuclei (SABRE-SHEATH).[7] As shown in Scheme 1, the required hardware is relatively simple.

As a result of experimental simplicity and its promise, SABRE and SABRE-SHEATH are now attracting an increasing number of research groups contributing to its rapid development.[4, 7, 14–20] A milestone for SABRE was the transition from organic solvents to aqueous solutions, which was recently achieved for ^{1}H-SABRE.[21–24]

Still, for ^{1}H spin lattice relaxation times are relatively short and the substrate scope is limited. Direct polarization transfer to heteronuclei has not been demonstrated in aqueous environment. Hyperpolarizing nitrogen-15 via SABRE-SHEATH allows a wider range of structural motives and relaxation times are characteristically larger.

SABRE-SHEATH with ^{15}N targets is made accessible with the water soluble [IrCl(IDEG)(COD)] precatalyst (**1a**). As shown in Scheme 2 the precatalyst is converted to the catalytically active species (**1**) in presence of substrates under a hydrogen atmosphere.[21] At μT magnetic field hydride and ^{15}N energy levels match and the spin system coherently evolves with a rate given by J_{NH}-into ^{15}N-polarization on substrates.[25]

We investigate different molecular motifs found in medical drugs, biomolecules and molecular tags. Structural motifs could be readily translated from the established [IrCl(IMes)(COD)] system.[15, 26]

Pyridine (**2**), the canonical SABRE substrate,[4] was a logical first choice. Next, nitriles are often encountered in drugs,[27] polarize consistently well, tolerate complex backbones, and show large ^{15}N-SABRE-SHEATH enhancements, despite little to no ^{1}H-SABRE.[26, 28] We selected benzonitrile (**3**) and α-cyano-4-hydroxycinnamic acid (**4**) (CHCA, buffered with NaOD to pH 7.5). Diazirines, which also do not exhibit ^{1}H enhancements, are common biomolecular tags that can replace CH_2 groups in many classes of biomolecules.[29] Here we use 2-cyano-3-(D_3-methyl-$^{15}N_2$-diazirine)-propanoic acid (**5**). Lastly, we focus on nicotinamide (**6**), the amide of vitamin B_3, which could be tolerated *in vivo* at detectable concentrations and is a potential option for translation to biomedical studies.[19, 30]

For these substrates we detail hyperpolarization levels, carefully characterize temperature and magnetic field dependencies, consider the effect of deuterated *vs* protonated solvents (D_2O *vs* H_2O), and measure relaxation time constants at various magnetic fields.

Results & Discussion

In Figure 1 we show a comparison between single scan spectra originating from compounds directly SABRE-SHEATH hyperpolarized in aqueous medium, referenced to thermally polarized neat ^{15}N-pyridine at 8.45 T. Concentrations of investigated compounds are different as a result of solubility as well as sample loss phenomena for benzonitrile and pyridine. Both pyridine and benzonitrile were initially prepared as 100 mM solutions but after activation by H_2 bubbling the concentrations were significantly reduced.

A synopsis of experimental results and conditions is given in Table 1 (experimental details provided in Materials and Methods). Spectra are acquired at 1 T and 8.45 T (see Scheme 1.) to study the field dependence of T_1 relaxation as detailed below. The 1 T measurements also demonstrate the feasibility of high sensitivity single scan ^{15}N detection with a benchtop NMR system. Furthermore, to determine the effect of proton containing solvents, nicotinamide was investigated in H_2O.

We find that polarization levels in deuterated solvents are largely independent of the detection field *i.e.* enhancements simply scale with the thermal polarization. In contrast, for nicotinamide in H_2O (Table 1, Entry 6), we observe lower apparent polarization levels at 8.45 T. This is caused by relaxation losses during transfer because it takes much longer to transfer the sample into the high field magnet (~8 s) than into the benchtop device sitting right next to the magnetic shields (~2 s). The solvent protons (and deuterons) are in chemical exchange with the ^{15}N-substrate where they cause spin-dipole relaxation. This relaxation mechanism scales with the distance between the relaxation partners r_{ij}^{-6} as well as the gyromagnetic ratio, which is 6.5 times smaller for deuterium,[3132] explaining the observed differences between solvents.

SABRE-SHEATH in water gives rise to a new set of challenges. Water has significantly higher viscosity and surface tension than methanol, and at room temperature the solubility of

hydrogen in water is five times lower.[33–34] We observed that some samples, specifically non-polar liquid state substrates (e.g. benzonitrile and pyridine) are extracted from the solvent when bubbling with hydrogen during the polarization buildup. Nicotinamide and CHCA, both crystalline solids when isolated, were used for systematic studies as substrate loss did not occur.[19]

Of particular interest are the dependence of the ^{15}N polarization on temperature and magnetic evolution field B_{evo}. Figure 2 contrasts the established [IrCl(IMes)(COD)] in methanol and catalyst (1) in H_2O/D_2O as a function of these variables (T, B_{evo}).

The temperature dependence was studied using a 100 mM nicotinamide sample. For catalyst system (1) in H_2O (Fig. 2A) and D_2O (Fig. 2B) the ^{15}N polarization increases with temperature. In contrast, in methanol (Fig. 2C, [IrCl(IMes)(COD)] precursor) the largest polarization is recorded at room temperature.

The magnetic field dependence is shown in Figure 2D. We compare normalized data (max. ^{15}N polarization: 0.13% in D_2O, 1.7% in MeOH-d4) of two nitrile/solvent systems: first, in blue: ^{15}N-acetonitrile in MeOH-d_4 with [IrCl(IMes)(COD)] and second, in magenta, ^{15}N-CHCA in D_2O with[IrCl(IDEG)(COD)] (**1a**).

We note that nitriles are better suited for this study than nicotinamide, as enhancements are more robust and reproducible. Additionally, they exhibit inversion of the NMR signal upon inversion of B_{evo}. Variation of the temperature changes the dissociation rate constants of substrate and catalyst bound H_2.[13, 15, 35] Optimal polarization transfer efficiency is expected when the exchange rate k_{diss} is on the order of the ^{15}N-to-hydride J_{NH}-coupling across the iridium center (see scheme 2).[13, 35] Figures 1A–C show that the IMes catalyst in methanol yields largest ^{15}N-polarization at room temperature, whereas catalyst (**1**) requires significantly elevated temperatures to achieve comparable exchange rates leading to maximum polarization. Based on these insights it is reasonable to expect ^{15}N polarization in water to decrease at even higher temperatures in analogy to methanol, as shown in Fig. 2C.

As seen in Fig. 2D, the methanol and water systems show very similar responses to B_{evo} at their respective optimized temperatures (22 °C and 72 °C). The response curves originate from two distinct matching conditions associated with overpopulation in ^{15}N-α or ^{15}N-β, giving either positive or negative NMR signal with identical polarization levels.[26] The matching conditions are given by[7]

$$B_{evo} = \pm \frac{J_{HH} + J_{NH}/2}{\gamma_H - \gamma_N} \quad \text{(Eq. 1)}$$

where J_{HH} is the hydride-to-hydride J-coupling (~ 10 Hz) and J_{NH} the hydride to ^{15}N coupling (~ 20 Hz) in (**1**). Experimentally, we observe maxima at $B_{evo} \approx \pm 0.5$ μT which is slightly higher than the ±0.3 μT predicted from Eq. 1, as the limited lifetime broadens the matching conditions.

Taken together, the observations of Fig. 1 (A–D) suggest, that the activation energy of substrate dissociation from (**1**) is significantly larger than for the established [IrCl(IMes)(COD)]-methanol systems. This is also supported by the fact that catalyst (**1**) in methanol at RT did not yield any enhancement.

The absolute polarization level in D_2O is about one order of magnitude smaller than for the methanol system, when compared at their respective optimized temperatures (^{15}N-CHCA in D_2O, $P(^{15}N)$ = 0.13 %, ^{15}N-CH_3CN in d4-MeOH, $P(^{15}N)$ = 1.7 %). Interestingly, this difference in hyperpolarization level can simply be attributed to the difference in hydrogen solubility (factor 5) and the difference in solvent concentration ($c(H_2O)$ = 55 mol/L, c(MeOH) = 28 mol/L, factor 2).

Current experimental data and theoretical considerations indicate that SABRE polarization levels are limited by the exchange of hydrides on the iridium center and the exchange kinetics of other ligand types (substrate/solvent), as well as both pressure and flow rate of *para*-hydrogen. Exchange of hydrogen restores the polarization source to the active complex species and process proceeds via the mixed classical non-classical hydride [$Ir(H)_2(\eta$-$H_2)$(IMes)L_2], with arbitrary ligands L.[13, 15] Formation of this species requires collision between a 16-electron complex and a hydrogen molecule, where collision with a *para*-hydrogen molecule may refresh the active species. As a result, the polarization is proportional to the concentration of *para*-hydrogen in solution, not the saturation concentration of hydrogen (*ortho* + *para*). Accordingly pressure dependence of polarizations is relatively weak, whereas dependence on the flow rate is significant. Depending on system composition a linear or exponential dependence of ^{15}N polarization on the flow rate was reported.[26, 36–37] We conclude the *para*-hydrogen enrichment in solution is limited by the exchange at the gas-liquid interface.

Let us now consider the substrate exchange process. The rates of ligand dissociation k_{diss} and association k_{asso} determine not only the lifetime of the complex where polarization transfer from the hydrides to the target nuclei occurs, but also the concentration of the 16-electron species required for the hydride exchange.[13] As a result ^{15}N polarization depends directly on the concentration of the 16-electron species. Accordingly, largest polarizations are observed at relatively low catalyst concentrations and high catalyst loadings. It is noteworthy that an exponential dependence of polarization on the substrate concentrations has been observed by Appleby et al.[38]

We point out that all reported polarization levels are not optimized with respect to sample composition, concentrations, hydrogen pressure or flow rate. Optimization of catalyst concentration and loading afforded an 8–10-fold increase of ^{15}N polarization level for the methanol system. Maximum polarizations are recorded at low catalyst concentrations and high catalyst loadings (^{15}N-nicotinamide $P(^{15}N)$ = 7 % ^{15}N-benzonitrile $P(^{15}N)$ = 16 %, metronidazole at natural abundance $P(^{15}N)$ = 20%).[7, 13, 17, 36, 39] We conclude, that ^{15}N polarization can be increased by at least a factor 10 by using low substrate concentrations and high catalyst loading. Further improvements are expected by modifications to the

experimental setup to allow for more effective mixing of hydrogen and solvent at higher pressures.

^{15}N Relaxation times in water

Of particular importance for hyperpolarization applications is the spin lattice relaxation time T_1, which defines the viable time delay between preparation of hyperpolarization and detection. We examined the T_1 lifetime for ^{15}N-Nicotinamide[39] and ^{15}N-CHCA, which constitute biocompatible compounds and contain ^{15}N in chemically different environments.[39–41] Table 2 shows the ^{15}N-T_1 relaxation times in D_2O, which at 1 T exceed 1 min for both compounds.

For ^{15}N-Nicotinamide at 8.45 T we find the effect of proton containing solvent (H_2O) on the T_1 time to be negligible. It should be noted that the ^{15}N T_1 time of nicotinamide at 8.45 T and room temperature is close to the T_1 reported for ^{13}C in the ^{13}C(1)-pyruvate markers currently in clinical use for prostate cancer diagnostics (T_1 = 29.2 s in-vivo, T_1 = 60 s, ex-vivo, 3 T).[8–9] It is noteworthy, that the ^{13}C T_1 values in-vivo are smaller than ex-vivo, characteristic for diffusion in constricted environments.

To elucidate this field dependence in more detail we hyperpolarized ^{15}N-CHCA and held the sample at different fields for variable times prior to detection. The results are shown in Fig. 3 displaying ^{15}N-relaxation time of CHCA (50 mM, pH 7.5, D_2O) at with different magnetic fields. For this compound relatively low magnetic fields of about 0.2 T give the longest relaxation times. This is an intriguing finding in the context of low-field approaches to NMR and MRI[42–43], which could be coupled with SABRE to establish low-cost spectroscopy and molecular imaging.

The scaling of signal-to-noise with magnetic field strongly depends on the exact experimental conditions. For traditional thermal NMR, signal is proportional to polarization and the induction. Both terms are proportional to B_0, thus the signal scales with B_0^2.[31, 44] In NMR, coil noise is typically dominant, which scales as $B_0^{1/4}$, hence signal-to-noise (S/N) is proportional to $B_0^{7/4}$.[44–46] However, with a hyperpolarized sample spin polarization is independent of B_0 and thus, S/N scales with $B_0^{3/4}$.

Another scenario arises for human MRI. Here, dielectric losses dominate, which are proportional to B_0. Thus S/N only increases proportional to B_0 for thermal MRI experiments.[45, 47] Therefore, S/N is expected to be independent of B_0 for hyperpolarized human MRI.[48–49] MRI in low magnetic fields has significant advantages, as magnet and RF-circuit design are flexible, easy to construct, and relatively inexpensive.[49–50] For example, high performance ^{1}H-MRI at 6.5 mT with thermal magnetization has already been reported.[42] It is noteworthy that recent advances in the low field domain, such as “External High-Quality-factor-Enhanced NMR” (EHQE-NMR)[51] and others[52] lead S/N independent of B_0 even for spectroscopic applications.

Materials and Methods

Solutions of substrates in D_2O/H_2O were added to [IrCl(IDEG)(COD)] (IDEG = 1,3-bis-(3,4,5-tris(diethyleneglycol)benzyl))imidazole-2-ylidene), COD = 1,5-cyclooctadiene), stirred until a homogeneous solution of known concentration in catalyst is obtained, and transferred to a 5 mm medium wall pressure NMR tube (Wilmad 524-PV-7). The typical sample volume was 350 μL. The solution was bubbled with argon for 30 minutes, pressurized with 10 bar of *para*-H_2 and hydrogen flow adjusted to obtain adequate bubbling. Catalyst activation times were 0.25–12 h depending on substrate, solvent (deuterated solvents require longer activation times), and temperature. Catalyst activation can be sped up significantly by raising temperature. For SABRE SHEATH experiments *para*-H_2 (Bruker BPHG 090, 38 K, 90%) was bubbled through a sample placed in a μT magnetic field. Hyperpolarization buildup is achieved in 0.5–2 min. The μT field is generated by a small solenoid inside a magnetic shield (see Scheme 1). The sample temperature was controlled with a water bath inside the magnetic shields. Measurements were performed with a Bruker Avance DX 360 (8.45 T) or Magritek Spinsolve $^1H/^{15}N$ Spectrometer (1 T). Enhancements are calculated relative to neat ^{15}N labeled pyridine. The concentration in the samples was monitored by ^1H spectroscopy.

Conclusions

We have demonstrated SABRE SHEATH hyperpolarization of 15N in aqueous media at moderate temperatures (20 – 80 °C) and achieve up to 1000-fold enhancements over thermal measurements at 8.45 T. We applied SABRE-SHEATH in water to biocompatible marker groups in different molecules (CHCA, nicotinamide, diazirine-moieties). Hyperpolarization of ^{15}N-nitrile and the $^{15}N2$-diazirine exemplifies how SABRE-SHEATH is amendable to more substrate classes because ^{15}N is closer to the hyperpolarization source than protons in the molecular backbone.

Furthermore, we demonstrated T_1 times comparable to, or exceeding, clinically used DNP tracers.[8–9] For example, nicotinamide in D_2O exhibits a ^{15}N relaxation time of 2 min, which is significantly longer than typical ^1H-T_1 (seconds) of traditional ^1H-SABRE substrates. Still, recent advances have demonstrated long lived ^1H singlet states with decay times of up to 4.5 min.[30] When such strategies are translated to ^{15}N, lifetimes in excess of 20 min become available.[53]

Imaging applications of SABRE hyperpolarized protons[24] as well as nitrogen-15 have already been reported.[36] Hyperpolarized heteronuclei are beneficial as they are background free and have a large chemical shift range which allows for easy chemical identification. Future developments may be expected to advance SABRE to in vivo molecular imaging complementing DNP-hyperpolarized ^{13}C tracers, which have quickly become an essential and routine tool giving detailed and fundamental insight into in vivo metabolism and biochemistry.[8–9, 54–58]

Supplementary Material

Refer to Web version on PubMed Central for supplementary material.

Acknowledgments

The authors gratefully acknowledge the NSF (CHE-1363008 and CHE-1416268), NIH 1R21EB018014, P41 EB015897 and 1R21EB020323, DOD CDMRP W81XWH-15-1-0271 and W81XWH-12-1-0159/BC112431, and Duke University for financial support of this research. This work has been supported by Deutsche Forschungsgemeinschaft (DFG-BL231/47-1), as well as by the European Union and the provinces of Gelderland and Overijssel (NL) through the EFRO Ultrasense NMR project. The authors gratefully acknowledge Magritek for supply of the 1 T ^{15}N-spectrometer and friendly technical assistance.

References

1. Carver TR, Slichter CP. Phys. Rev. 1956; 102:975–980.
2. Cudalbu C, Comment A, Kurdzesau F, van Heeswijk RB, Uffmann K, Jannin S, Denisov V, Kirik D, Gruetter R. Phys. Chem. Chem. Phys. 2010; 12:5818–5823. [PubMed: 20461252]
3. Shchepin RV, Coffey AM, Waddell KW, Chekmenev EY. Anal. Chem. 2014; 86:5601–5605. [PubMed: 24738968]
4. Adams RW, Aguilar JA, Atkinson KD, Cowley MJ, Elliott PIP, Duckett SB, Green GGR, Khazal IG, Lopez-Serrano J, Williamson DC. Science. 2009; 323:1708–1711. [PubMed: 19325111]
5. Bowers CR, Weitekamp DP. Phys. Rev. Lett. 1986; 57:2645–2648. [PubMed: 10033824]
6. Ben-Amar Baranga A, Appelt S, Romalis MV, Erickson CJ, Young AR, Cates GD, Happer W. Phys. Rev. Lett. 1998; 80:2801–2804.
7. Theis T, Truong ML, Coffey AM, Shchepin RV, Waddell KW, Shi F, Goodson BM, Warren WS, Chekmenev EY. J. Am. Chem. Soc. 2015; 137:1404–1407. [PubMed: 25583142]
8. Kurhanewicz J, Vigneron DB, Brindle K, Chekmenev EY, Comment A, Cunningham CH, DeBerardinis RJ, Green GG, Leach MO, Rajan SS, Rizi RR, Ross BD, Warren WS, Malloy CR. Neoplasia. 2011; 13:81–97. [PubMed: 21403835]
9. Nelson SJ, Kurhanewicz J, Vigneron DB, Larson PEZ, Harzstark AL, Ferrone M, van Criekinge M, Chang JW, Bok R, Park I, Reed G, Carvajal L, Small EJ, Munster P, Weinberg VK, Ardenkjaer-Larsen JH, Chen AP, Hurd RE, Odegardstuen LI, Robb FJ, Tropp J, Murray JA. Sci. Transl. Med. 2013; 5:198ra108–198ra108.
10. Eshuis N, van Weerdenburg BJA, Feiters MC, Rutjes FPJT, Wijmenga SS, Tessari M. Angew. Chem. Int. Ed. 2015; 54:1372–1372.
11. Eshuis N, Hermkens N, van Weerdenburg BJA, Feiters MC, Rutjes FPJT, Wijmenga SS, Tessari M. J. Am. Chem. Soc. 2014; 136:2695–2698. [PubMed: 24475903]
12. Hövener J-B, Schwaderlapp N, Lickert T, Duckett SB, Mewis RE, Highton LAR, Kenny SM, Green GGR, Leibfritz D, Korvink JG, Hennig J, von Elverfeldt D. Nat. Comm. 2013; 4:2946.
13. Barskiy DA, Pravdivtsev AN, Ivanov KL, Kovtunov KV, Koptyug IV. Phys. Chem. Chem. Phys. 2015; 89:89–93.
14. Zeng H, Xu J, Gillen J, McMahon MT, Artemov D, Tyburn J-M, Lohman JAB, Mewis RE, Atkinson KD, Green GGR, Duckett SB, van Zijl PCM. J. Magn. Reson. 2013; 237:73–78. [PubMed: 24140625]
15. Cowley MJ, Adams RW, Atkinson KD, Cockett MCR, Duckett SB, Green GGR, Lohman JAB, Kerssebaum R, Kilgour D, Mewis RE. J. Am. Chem. Soc. 2011; 133:6134–6137. [PubMed: 21469642]
16. Theis T, Truong M, Coffey AM, Chekmenev EY, Warren WS. J. Magn. Reson. 2014; 248:23–26. [PubMed: 25299767]
17. Barskiy DA, Shchepin RV, Coffey AM, Theis T, Warren WS, Goodson BM, Chekmenev EY. J. Am. Chem. Soc. 2016; 138:8080–8083. [PubMed: 27321159]
18. Nikolaou P, Goodson BM, Chekmenev EY. Chem. Eur. J. 2015; 21:3156–3166. [PubMed: 25470566]
19. Shchepin RV, Barskiy DA, Coffey AM, Theis T, Shi F, Warren WS, Goodson BM, Chekmenev EY. ACS Sensors. 2016; 1:640–644. [PubMed: 27379344]
20. Shchepin RV, Chekmenev EY. J. Label. Compd. Rad. 2014; 57:621–624.

21. Spannring P, Reile I, Emondts M, Schleker PPM, Hermkens NKJ, van der Zwaluw NGJ, van Weerdenburg BJA, Tinnemans P, Tessari M, Blümich B, Rutjes FPJT, Feiters MC. Chem. Eur. J. 2016; 22:9277–9282. [PubMed: 27258850]
22. Truong ML, Shi F, He P, Yuan B, Plunkett KN, Coffey AM, Shchepin RV, Barskiy DA, Kovtunov KV, Koptyug IV, Waddell KW, Goodson BM, Chekmenev EY. J. Phys. Chem. B. 2014; 18:13882–13889.
23. Fekete M, Bayfield O, Duckett SB, Hart S, Mewis RE, Pridmore N, Rayner PJ, Whitwood A. Inorg. Chem. 2013; 52:13453–13461. [PubMed: 24215616]
24. Rovedo P, Knecht S, Bäumlisberger T, Cremer AL, Duckett SB, Mewis RE, Green GGR, Burns MJ, Rayner PJ, Leibfritz D, Korvink JG, Hennig J, Pütz G, von Elverfeldt D, Hövener J-B. J. Phys. Chem. B. 2016; 120:5670–5677. [PubMed: 27228166]
25. Barskiy DA, Pravdivtsev AN, Ivanov KL, Kovtunov KV, Koptyug IV. Simple analytical model for Signal Amplification by Reversible Exchange (SABRE) process. Phys. Chem. Chem. Phys. 2015; 18:89–93. [PubMed: 26645782]
26. Colell JFP, Logan AWJ, Zhou Z, Shchepin RV, Barskiy DA, Ortiz GX, Wang Q, Malcolmson SJ, Chekmenev EY, Warren WS, Theis T. The Journal of Physical Chemistry C, Article ASAP. 2017; doi: 10.1021/acs.jpcc.6b12097
27. Fleming FF, Yao L, Ravikumar PC, Funk L, Shook BC. J. Med. Chem. 2010; 53:7902–7917. [PubMed: 20804202]
28. Mewis RE, Green RA, Cockett MCR, Cowley MJ, Duckett SB, Green GGR, John RO, Rayner PJ, Williamson DC. J. Phys. Chem. B. 2015; 119:1416–1424. [PubMed: 25539423]
29. Dubinsky L, Krom BP, Meijler MM. Bioorg. Med. Chem. 2012; 20:554–570. [PubMed: 21778062]
30. Roy SS, Norcott P, Rayner PJ, Green GGR, Duckett SB. Angew. Chem. Int. Ed. 2016; 55:15642–15645.
31. Abragam, A. The principles of nuclear magnetism. Oxford: Clarendon Press; 1961.
32. Halbach K. Nucl. Instr. Meth. 1980; 169:1–10.
33. Crozier TE, Yamamoto S. J. Chem. Eng. Data. 1974; 19:242–244.
34. Brunner E. J. Chem. Eng. Data. 1985; 30:269–273.
35. Knecht S, Pravdivtsev AN, Hövener J-B, Yurkovskaya AV, Ivanov KL. RSC. Adv. 2016; 6:24470–24477.
36. Truong ML, Theis T, Coffey AM, Shchepin RV, Waddell KW, Shi F, Goodson BM, Warren WS, Chekmenev EY. J. Phys. Chem. C. 2015; 119:8786–8797.
37. Shchepin RV, Truong ML, Theis T, Coffey AM, Shi F, Waddell KW, Warren WS, Goodson BM, Chekmenev EY. J. Phys. Chem. Lett. 2015; 6:1961–1967. [PubMed: 26029349]
38. Appleby KM, Mewis RE, Olaru AM, Green GGR, Fairlamb IJS, Duckett SB. Chem. Sci. 2015; 6:3981–3993.
39. Shchepin RV, Barskiy DA, Mikhaylov DM, Chekmenev EY. Bioconjugate Chem. 2016; 27:878–882.
40. Wang H, Lanks KW. Cancer Research. 1986; 46:5349–5352. [PubMed: 3756884]
41. Olaru AM, Burns MJ, Green GGR, Duckett SB. Chem. Sci. 2016; 8:2257–2266. [PubMed: 28507682]
42. Sarracanie M, LaPierre CD, Salameh N, Waddington DEJ, Witzel T, Rosen MS. Sci. Rep. 2015; 5:15177. [PubMed: 26469756]
43. Danieli E, Mauler J, Perlo J, Blümich B, Casanova F. J. Magn. Reson. 2009; 198:80–87. [PubMed: 19217330]
44. Hoult DI, Richards RE. J. Magn. Reson. 1976; 24:71–85.
45. Hoult DI, Lauterbur PC. J. Magn. Reson. 1979; 34:425–433.
46. Hoult, DI. eMagRes. John Wiley & Sons, Ltd; 2007. Sensitivity of the NMR Experiment.
47. Hoult DI. Enc. Magn. Reson. 2007; doi: 10.1002/9780470034590.emrstm0491
48. Hoult DI, Richards RE. J. Magn. Reson. 1976; 24:71–85.
49. Minard KR, Wind RA. Concepts Magn. Reson. 2001; 13:190–210.
50. Danieli E, Perlo J, Blümich B, Casanova F. Physical Review Letters. 2013; 110 180801-1-5.

51. Suefke M, Liebisch A, Blumich B, Appelt S. Nat. Phys. 2015; 11:767–771.
52. Coffey AM, Truong M, Chekmenev EY. J. Magn. Reson. 2013; 237:169–174. [PubMed: 24239701]
53. Theis T, Ortiz GX, Logan AWJ, Claytor KE, Feng Y, Huhn WP, Blum V, Malcolmson SJ, Chekmenev EY, Wang Q, Warren WS. Sci. Adv. 2016; 2:e1501438–e1501438. [PubMed: 27051867]
54. Nelson SJ, Kurhanewicz J, Vigneron DB, Larson PE, Harzstark AL, Ferrone M, van Criekinge M, Chang JW, Bok R, Park I, Reed G, Carvajal L, Small EJ, Munster P, Weinberg VK, Ardenkjaer-Larsen JH, Chen AP, Hurd RE, Odegardstuen LI, Robb FJ, Tropp J, Murray JA. Sci. Transl. Med. 2013; 5:198ra108.
55. Sriram R, Van Criekinge M, Hansen A, Wang ZJ, Vigneron DB, Wilson DM, Keshari KR, Kurhanewicz J. NMR Biomed. 2015; 28:1141–1149. [PubMed: 26202449]
56. Keshari KR, Sriram R, Van Criekinge M, Wilson DM, Wang ZJ, Vigneron DB, Peehl DM, Kurhanewicz J. The Prostate. 2013; 73:1171–1181. [PubMed: 23532911]
57. Rodrigues TB, Serrao EM, Kennedy BWC, Hu D-E, Kettunen MI, Brindle KM. Nat. Med. 2013; 20:93–97. [PubMed: 24317119]
58. Reile I, Eshuis N, Hermkens NKJ, van Weerdenburg BJA, Feiters MC, Rutjes FPJT, Tessari M. The Analyst. 2016; 141:4001–4005. [PubMed: 27221513]

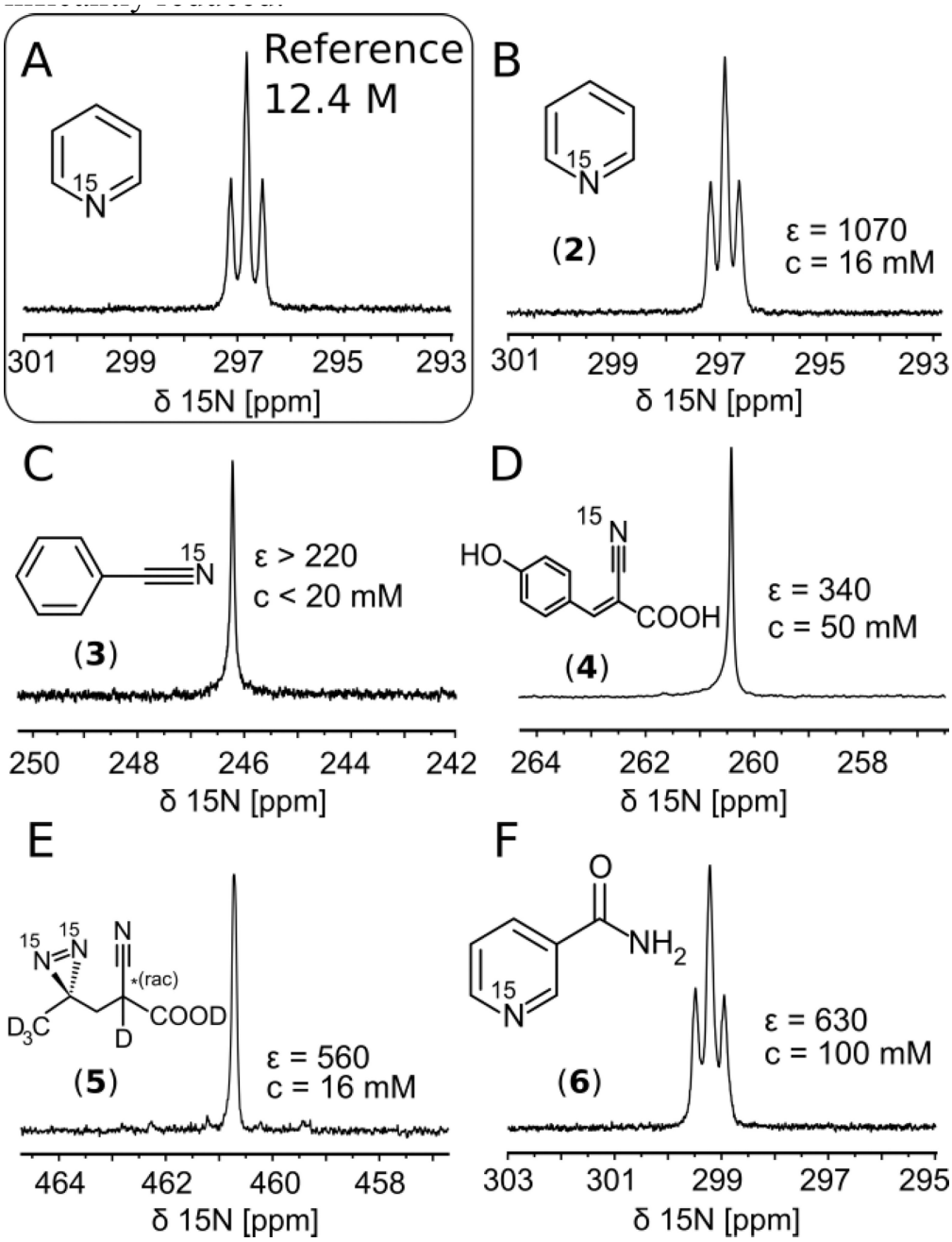

Figure 1.

^{15}N spectra of A) thermally polarized reference at 8.45 T and B–F) hyperpolarized compounds (in D_2O unless denoted otherwise). A) neat ^{15}N-pyridine. B) ^{15}N-Pyridine, C) ^{15}N-Benzonitrile, D) ^{15}N-CHCA, E) ^{15}N2-Diazirine F) ^{15}N-Nicotinamide (in H_2O).

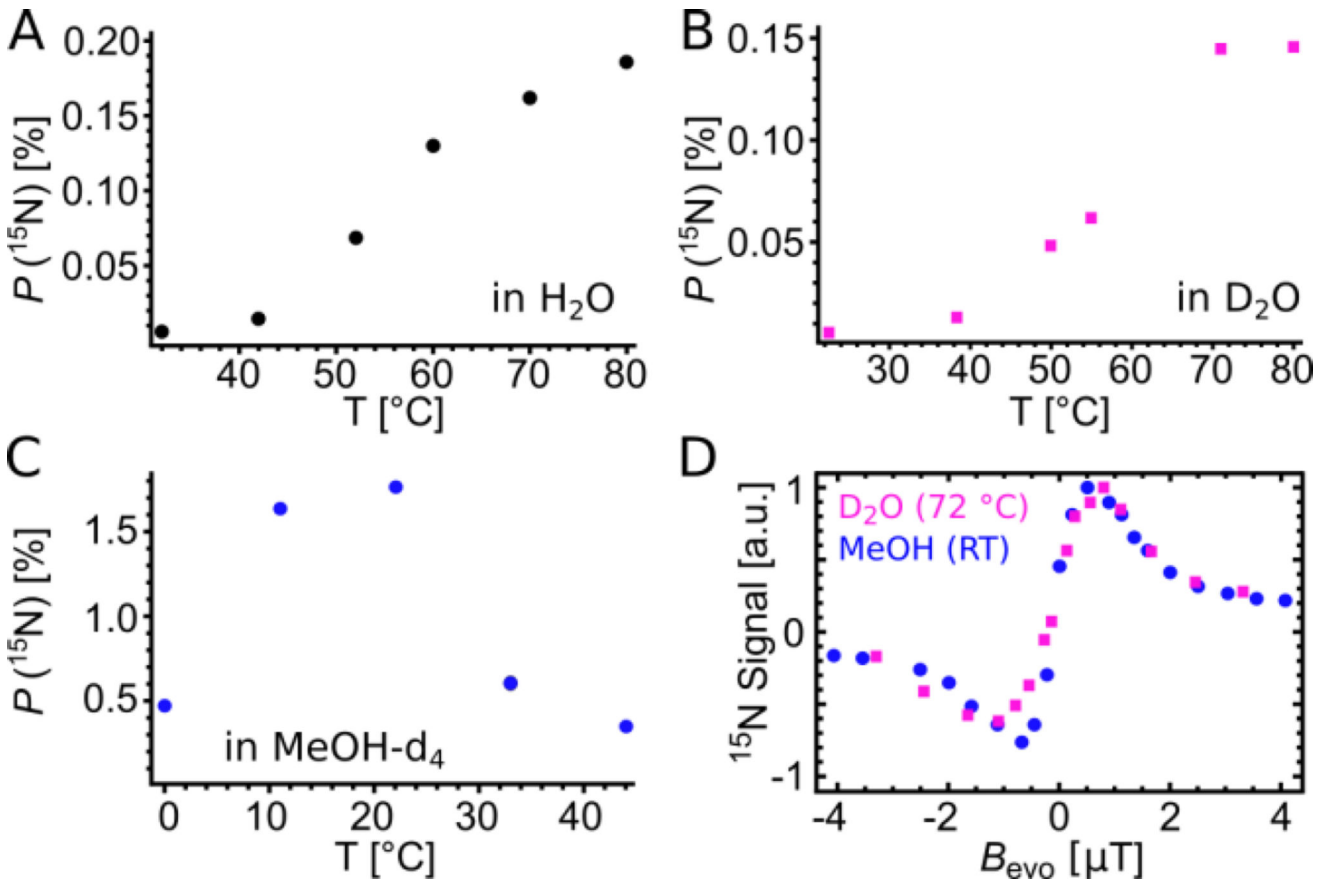

Figure 2.

Comparison of ^{15}N polarization as a function of temperature in A) H_2O, B) D_2O and C) methanol-d_4 at B_{evo} = 0.5 μT. D) Hyperpolarized signals as function of μT field at the temperature corresponding to maximum polarization in the respective solvents: 22 °C for ^{15}N-acetonitrile in MeOH-d_4 and 72 °C for ^{15}N-CHCA in D_2O (blue: 5 mM [IrCl(IMes)(COD)], 30 mM pyridine, 100 mM ^{15}N-CH_3CN, methanol-d4; magenta: 5mM [IrCl(IDEG)(COD)], 30 mM pyridine, 50 mM ^{15}N-CHCA, D_2O).

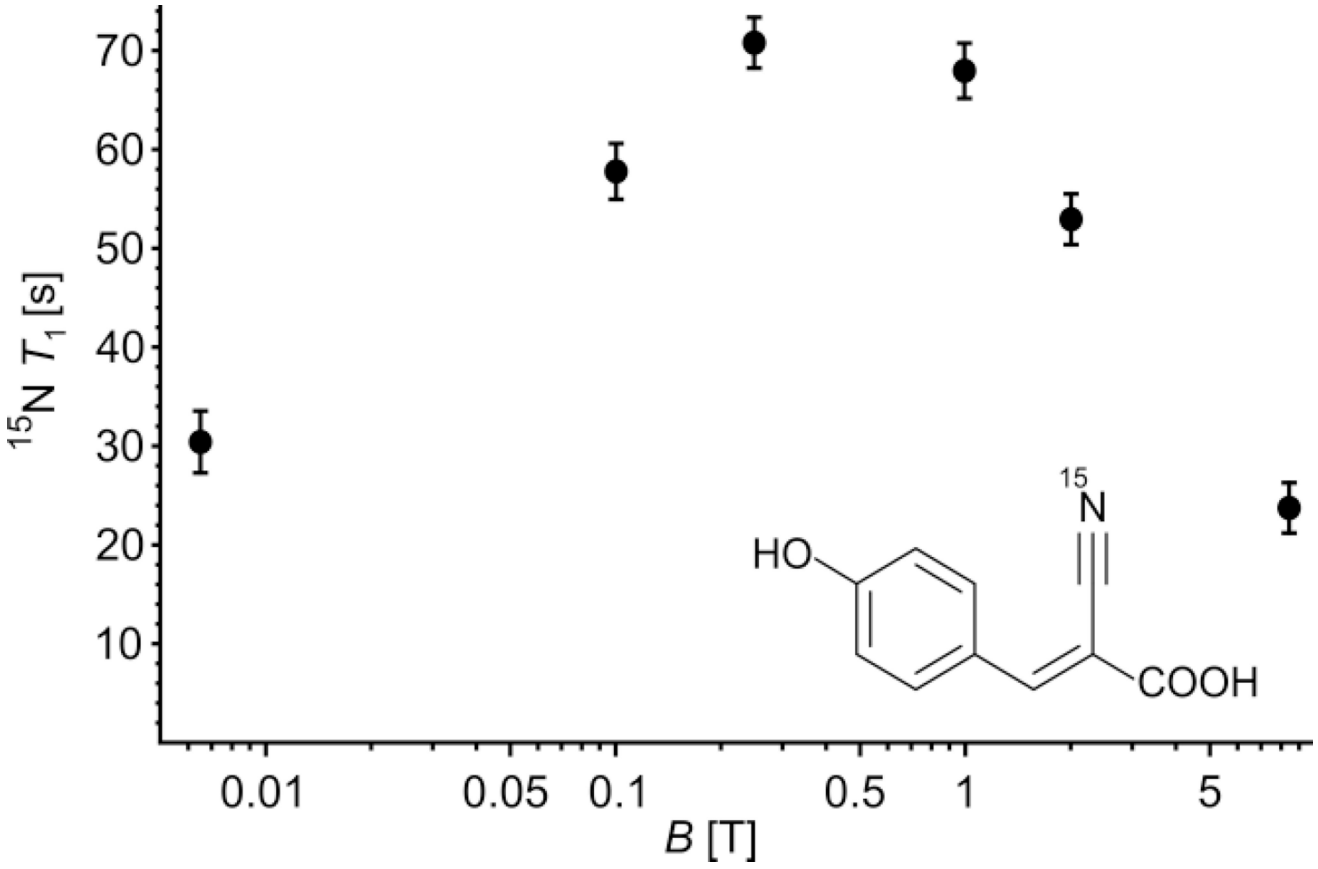

Figure 3.

^{15}N T_1 time constant of CHCA as a function of the magnetic field. The sample is hyperpolarized and stored at a given field for an incremented delay time and detected at 8.45 T.

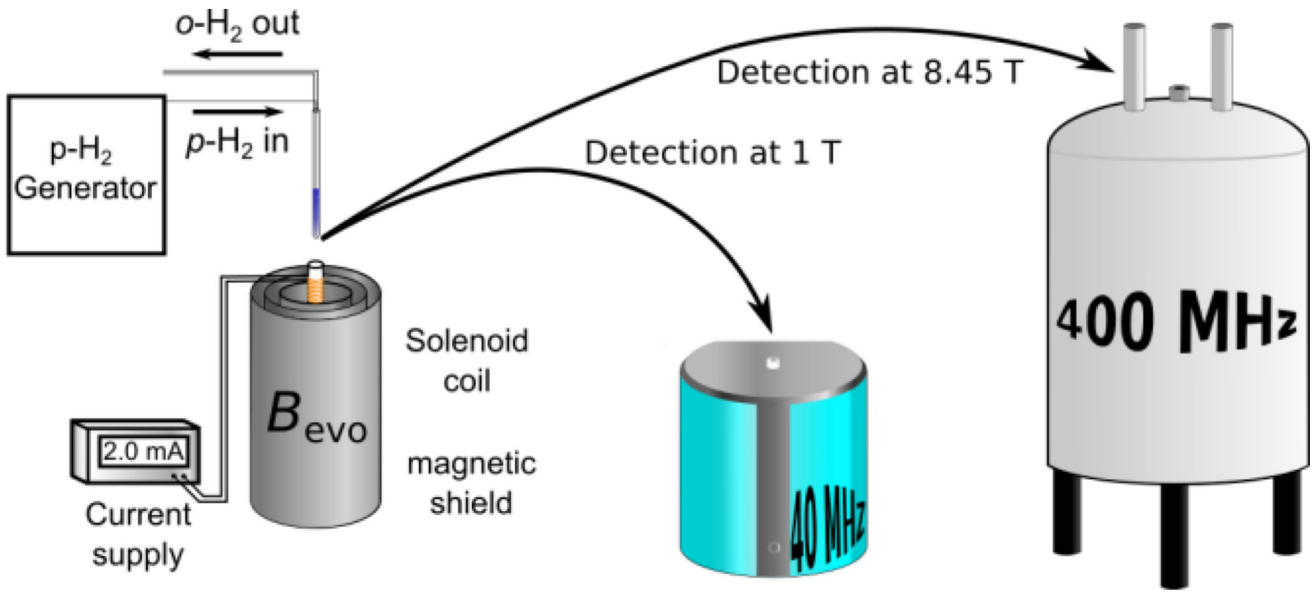

Scheme 1.

A sample is hyperpolarized *via* SABRE-SHEATH for an evolution time t_{evo} at optimized matching field B_{evo} of ~0.5 μT established by a small solenoid coil in a magnetic shield that attenuates the Earth's magnetic field. The sample is transferred into a benchtop (1 T) NMR spectrometer or conventional high-field (8.45 T) spectrometer for detection after hyperpolarization.

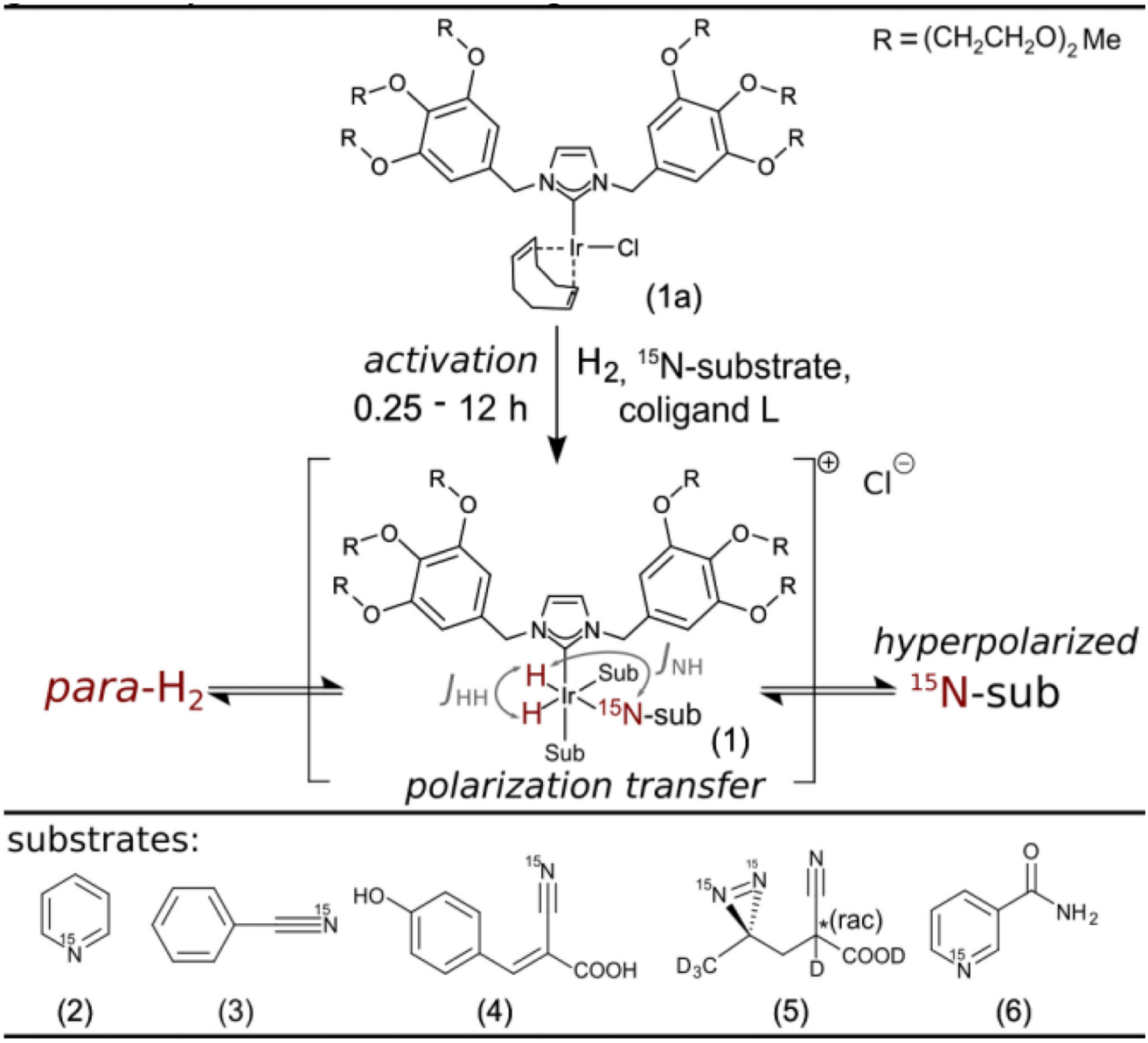

Scheme 2.

The precatalyst [IrCl(IDEG)(COD)] (1a) is transformed into the active species Ir(IDEG)$(H)_2Sub_3$ (Sub = Substrate) (**1**) in the presence of a substrate of choice (2–6) under a hydrogen atmosphere. Reversible exchange leads to polarization buildup on ^{15}N within 30–120 s. The polarization transfer is primarily driven by the J_{NH}-coupling through the bonds that form a 180° angle. The N-H coupling through bonds forming a 90° angle is close to zero.

Table 1

Synopsis of experimental conditions, enhancements and polarization levels. Substrates are ^{15}N labelled, solvent is D_2O unless otherwise specified. Concentrations of liquid substrates are determined at the time of the experiment using ^{1}H spectroscopy. T = 75 °C.

Substrate	Activation time [h]	$c_{substrate}/c_{catalyst}$	$c_{Substrate}$ [mM]	Enhancement 8.45 T (P [%])	Enhancement 1 T (P [%])	Enhancement ratio (1 T/8.45 T)
(**2**) pyridine	12	3.3	16.5[b]	1100	_[c]	_[c]
(**3**) benzonitrile	0.25	20	50[a,b]	90	_[c]	_[c]
(**4**) CHCA	12	10	50	440 (0.13)	3700 (0.13)	8.4
(**5**) diazirine	6	10	16.3	560 (0.16)	4700 (0.17)	8.4
(**6**) nicotinamide	12	20	100	520(0.16)	6100 (0.21)	8.9
(**6**) nicotinamide H_2O	12	20	100	630 (0.2)	10500 (0.37)	28

[a] Signal maximum obtained 30 min. after activation, subsequent substrate loss due to evaporation.

[b] Initial concentration 100 mM.

[c] Insufficient SNR.

J Am Chem Soc. Author manuscript; available in PMC 2018 June 14.

Table 2

^{15}N T_1 times of 100 mM Nicotinamide and 50 mM CHCA in D_2O at different detection fields.

	T_1 [s] 1 T	T_1 [s] 8.45 T
^{15}N-CHCA	71 ± 15[a]	24 ± 3
^{15}N-Nicotinamide	116 ± 10	32[b] ± 4

[a] detected and stored at 1 T. Control by detection at 8.45 T: T_1 = 68 ± 2 s.

[b] In H_2O: 32 ± 5.5 s